EMISSION MÖSSBAUER STUDY OF RECOIL-INDUCED FRENKEL PAIRS IN NICKEL CREATED BY NEUTRINO AND GAMMA-RAY EMISSION IN THE ELECTRON CAPTURE DECAY OF ^{57}Ni

M. DEVILLERS, J. LADRIERE and D. APERS

Laboratoire de Chimie Inorganique et Nucléaire, Université de Louvain, Chemin du Cyclotron, 2, B-1348 Louvain-la-Neuve, Belgium

Received 21 April 1986

Internal radiation effects of the ^{57}Ni → ^{57}Co → ^{57}Fe double decay are investigated by means of ^{57}Fe Mössbauer emission spectroscopy in ^{57}Ni-labelled metallic nickel. The recoil of ^{57}Co atoms due to neutrino and high-energy γ-ray emission has been detected at low temperature. According to the replacement collision mechanism, recoil atoms are located in two different vacancy-associated substitutional positions. The experimental results and the subsequently proposed recoil model for the ^{57}Co nucleogenic atoms agree perfectly well with the observations of the external irradiation effects in metals; this agreement between internal and external radiation damage concerns the displacement threshold energy and the recoil anisotropy, as well as the recovery mechanism.

1. Introduction

Because of their technological interest, metals and alloys have been considered for a long time as appropriate systems to study radiative defects induced by nuclear transformations or by external irradiation with neutrons or charged particles. More thorough investigations are made possible by the development of several complementary physical methods (Mössbauer spectroscopy, perturbed angular correlation (PAC), positron annihilation) which provide, at specific levels, a means of characterization of the structural and electronic perturbations in the solid state [1–4].

In the present work, ^{57}Fe Mössbauer emission spectroscopy is used for an "in situ" observation of the internal radiation damage provoked by the cumulative ^{57}Ni (T = 36.0 h, β^+ and EC) and ^{57}Co (T = 270 d, EC) decays in a ^{57}Ni-labelled nickel metal host. As a survey of the energetic aspects will show hereafter, the recoil energies available during the first decay of ^{57}Ni into ^{57}Co lie above the typical displacement threshold energy values accepted for crystalline material ($E_d \cong 25$ eV), whereas no displacement can occur during the subsequent decay of ^{57}Co into ^{57}Fe. Therefore, nucleogenic ^{57}Co atoms, and consequently the ultimate ^{57}Fe species, may be located in unusual configurations which are not expected to appear in corresponding ^{57}Co-labelled compounds.

In a metallic lattice, the electrical conduction properties mask the electronic effects due to the Auger cascade (10^{-15} s) before the Mössbauer radiation is emitted ($\tau \cong 10^{-7}$ s). Together with the lack of any other self-radiolytic effect, this means that only mechanical effects due to a recoil displacement in the matrix have to be taken into account.

2. Energetics

A simplified disintegration scheme of ^{57}Ni and ^{57}Co is presented in fig. 1 [5]. Table 1 summarizes the free atom recoil energy values associated with the individual steps of these nuclear transitions.

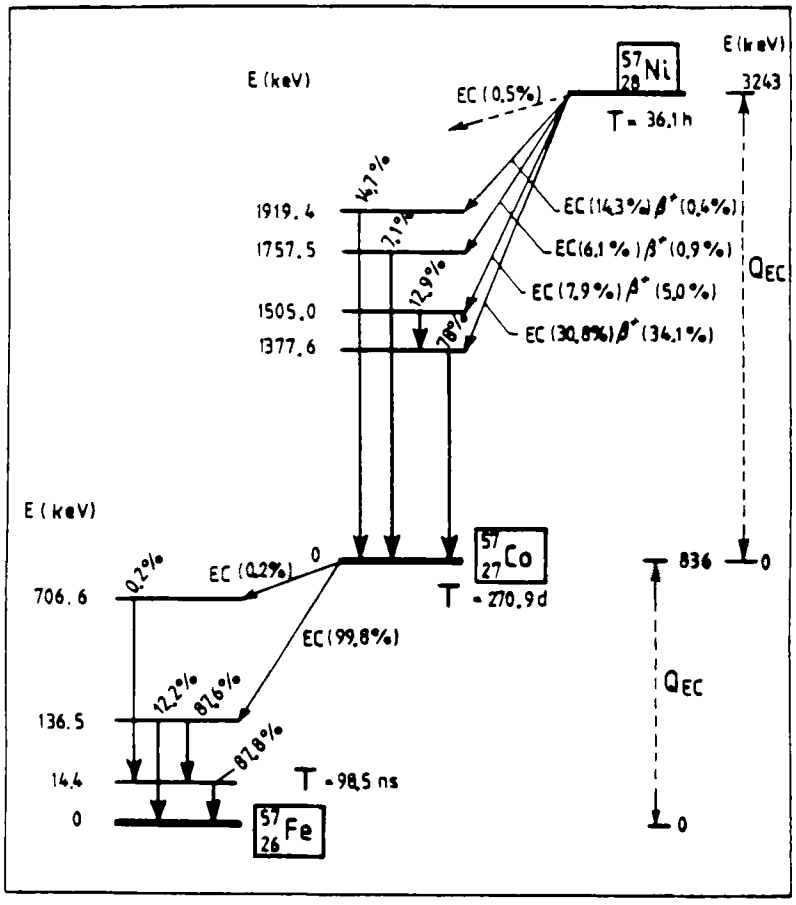

Fig. 1. Decay scheme of ^{57}Ni and ^{57}Co.

Table 1

Free-atom recoil energies (E_R) associated with the individual processes of the ^{57}Ni and ^{57}Co decays

Parent isotope	Decay mode	Emitted particle	Energy (keV)	E_R (eV)	Intensity (%)
^{57}Ni	EC (59.6%)	ν	1316[a]	16.3	14.3
			1478	20.6	6.1
			1730	28.2	7.9
			1858	32.5	30.8
	β^+ (40.4%)	β^+ [d]	$\leqslant$ 302[b]	$\leqslant$ 3.8[b]	0.4[c]
			$\leqslant$ 463	$\leqslant$ 6.5	0.9
			$\leqslant$ 716	$\leqslant$ 11.7	5.0
			$\leqslant$ 843	$\leqslant$ 14.8	34.1
		ν [e]	$\leqslant$ 843	$\leqslant$ 6.7	-
		$\beta^+ + \nu$ [f]	$\Sigma \leqslant$ 843	$\leqslant$ 13.1[g]	-
	EC/β^+	γ	127.4	0.15	12.9
			1377.6	17.9	78
			1757.5	29.1	7.1
			1919.4	34.7	14.7
^{57}Co	EC (100%)	ν	693[h]	4.5	100
		γ	14.4	0.002	9.5
			122.1	0.14	85.6
			136.5	0.17	10.6
			692.2	4.5	0.2
		ce	$\leqslant$ 135	$\leqslant$ 1.5	-

[a] For K-capture ($EC_L/EC_K = 0.1$).
[b] Maximum values of E_{β^+} and corresponding E_R.
[c] Total intensity for β^+ decay to a given nuclear level (absolute intensity for 100 decays of ^{57}Ni).
[d] Hypothesis of a neutrino emitted at rest.
[e] Hypothesis of a positron emitted at rest.
[f] Sharing of energy between positron and neutrino.
[g] Range of values depending on the angular correlation between the emission directions of both particles.
[h] Mean value.

According to the large total decay energy of ^{57}Ni atoms (Q = 3243 keV), the corresponding recoil energies sometimes exceed the displacement threshold energy E_d in nickel. By means of external irradiation of metals at low temperatures (4–20 K) with high-energy electrons (0.5–3 MeV), a mean value of E_d = 24 eV has first been proposed for Ni [6]. Further studies accounted for a strong anisotropy of this value with respect to the different crystallographic directions. In the case of Ni, reliable

results give E_d = 21 ± 1 eV for ⟨110⟩, E_d = 38 ± 3 eV for ⟨100⟩, and $E_d > 60$ eV for ⟨111⟩ directions [7]. Data from table 1 indicate that the maximum recoil energy of ^{57}Co atoms equals 35 eV (15%) and that $E_R \geqslant 25$ eV for 60% of the nuclear events. In any case, the recoil energy of the nucleogenic ^{57}Co atoms associated with an individual disintegration step exceeds 15 eV, whatever the decay mode of the ^{57}Ni parent atom be. On the other hand, the recoil energy of the ^{57}Fe atoms produced by the EC decay of ^{57}Co is in all cases too low for atomic displacement to occur. It will thus be admitted that the physico-chemical surroundings of the ^{57}Fe nucleogenic atoms actually reflect the consequences of the initial ^{57}Ni decay. It should however be remembered that the above mentioned values of a recoil energy associated with the ^{57}Ni decay have been obtained neglecting the possible additivity of recoil momenta, particularly in the case of $\beta-\gamma$ correlations.

Parallel investigations by Mössbauer emission spectroscopy on ^{57}Ni-labelled nickel (^{57}Ni : Ni), ^{57}Co-doped nickel (^{57}Co : Ni) and ^{57}Co-labelled cobalt samples (^{57}Co : Co) enable us to verify the existence of such effects and to evaluate their magnitude.

3. Experimental

3.1. ^{57}Ni ACTIVITY

Production of the initial ^{57}Ni activity through the ^{58}Ni (p, pn) ^{57}Ni reaction was achieved by irradiation of a natural nickel target with 30 MeV protons at the isochronal cyclotron at Louvain-la-Neuve. Typical yields are about 660 μCi/μA.h (24 MBq/μA.h) [8]. The target is dissolved in hot concentrated hydrochloric acid to which some drops of hydrogen peroxide have been added; the solution is passed through an anionic exchanger (Amberlite IRA-400) to separate ^{57}Ni from other contaminating radionuclides. Among the latter, ^{57}Co, directly produced by other nuclear reactions, is particularly unwanted because it interferes with the ^{57}Co daughter atoms arising from the ^{57}Ni EC or β^+ decay. Preliminary results showed that elution with HCl 10M allows the recovery of some 95% of the ^{57}Ni activity, while the decontamination has decreased ^{57}Co to only 0.01% of its initial amount.

3.2. SYNTHESIS OF THE LABELLED COMPOUNDS

A powdered sample of ^{57}Ni-labelled metallic nickel is obtained by thermal decomposition of ^{57}Ni : $NiC_2O_4.2H_2O$ above 400 °C under pure argon atmosphere. The dehydrated nickel(II) oxalate is synthesized by adding crushed oxalic acid in excess to a ^{57}Ni-containing aqueous solution of $NiCl_2$. The initial ^{57}Ni activity of the sample amounts to about 20 mCi (740 MBq), which will yield about 100 μCi (3.7 MBq) ^{57}Co.

^{57}Co-labelled or doped compounds and prepared in a similar way by thermal decomposition of the corresponding oxalates and formates (^{57}Co : $CoC_2O_4.2H_2O$; ^{57}Co : $Co(HCO_2)_2.2H_2O$; ^{57}Co : $NiC_2O_4.2H_2O$; ^{57}Co : $Ni_{1-x}Co_xC_2O_4.2H_2O$ with $x = 0.01$ and 0.001).

The nature of the thermolysis products has been verified by X-ray diffraction of the powder and, as it will be shown further, agrees well with the previously published Mössbauer parameters.

3.3. STORAGE, ANALYSIS AND DATA TREATMENT

After synthesis, the ^{57}Ni-labelled samples are stored in liquid nitrogen for 15 to 20 days in order to reduce annealing effects during the complete decay of ^{57}Ni into ^{57}Co. Mössbauer emission spectra are then registered at low temperatures (90 K) before and after warming to room temperature (RT). Subsequent measurements were performed at RT and at higher temperatures. The emission spectra are recorded using a constant acceleration transducer coupled with a multichannel ELSCINT-Promeda analyser; resonance is observed between the studied sample and a moving ^{57}Fe-enriched hexacyanoferrate(II) absorber (0.7 mg ^{57}Fe/cm^2; $\Gamma = 0.36 \pm 0.03$ mm.s^{-1}). All the isomer shifts mentioned in the text are relative to α-Fe metal at 295 K. Mossbauer data are resolved in Lorentzian lines using an iterative least-square fit procedure, controlled by a chi-square test. The velocity sign has been reversed in the emission spectra to allow direct comparison between emission and absorption data.

4. Results

4.1. ^{57}Fe IN Fe, Co AND Ni

The absorption Mössbauer spectra of ^{57}Fe in Fe, Co and Ni metals show the typical magnetic sextet due to the Zeeman interaction; the separation between the outermost resonance lines provide a direct measurement of the magnetic hyperfine field at the nucleus (at 295 K: 330, 310 and 265 kOe in Fe, Co and Ni, respectively [9]) and is related to the electronic structure of the host metal [10].

4.2. ^{57}Co IN Co AND Ni

Mössbauer emission parameters of ^{57}Fe in different samples of ^{57}Co : Co and ^{57}Co : Ni are listed in table 2. In agreement with the absence of electronic aftereffects in metals, the emission spectra of ^{57}Fe in ^{57}Co : Co and ^{57}Co : Ni do not significantly differ from the above described absorption spectra, except for a slight broadening of the lines at low temperature. Moreover, the line widths are dependent on the thermal treatment of the starting compound, which affects the granulometry of the sample. Such a broadening can appear as a result of local structural inhomogeneities inducing

Table 2

Emission Mössbauer parameters of ^{57}Fe in ^{57}Co-doped Co and Ni

Compound	Sample[a]	T_S (K)	δ^{Fe} (mm/s)	Γ (mm/s)	H (kOe)
^{57}Co : Co	I	90	0.11	0.55	329
		295	0.01	0.47	327
^{57}Co : Co	II	295	0.00	0.60	325
^{57}Co : Ni	III	90	0.09	0.78	289
		295	0.01	0.44	271
^{57}Co : Ni	IV	90	0.08	0.75	275
		295	0.00	0.48	264
^{57}Co : Ni	V	90	0.12	0.74	283
		295	0.00	0.61	267
^{57}Co : Ni + 1% Co	VI	295	− 0.01	0.53	270
^{57}Co : Ni + 0.1% Co	VII	295	− 0.01	0.48	269

[a] I : ^{57}Co : $CoC_2O_4.2H_2O$ heated at 550 °C under argon.
II : ^{57}Co : $Co(HCO_2)_2.2H_2O$ heated at 450 °C under nitrogen.
III : ^{57}Co : $NiC_2O_4.2H_2O$ heated at 550 °C under argon.
IV : ^{57}Co : $NiC_2O_4.2H_2O$ heated at 450 °C under argon.
V : ^{57}Ni : $NiC_2O_4.2H_2O$ heated at 500 °C under argon after three months decay.
VI-VII : ^{57}Co : $NiC_2O_4.2H_2O$ with 1 or 0.1% carrier Co heated at 450 °C under argon.

weak quadrupole splittings, as in ^{57}Fe : Cu-Ni [11]. Another interpretation may be found in a dispersion of the internal magnetic field values, arising from local composition heterogeneities. Such hypothesis has been advanced in the case of macroscopic mixtures of magnetically different elements, e.g. alloys of Fe and Cr, V, Si or Al [12]. In the present case, however, this explanation may quite probably be ruled out. Due to their similar magnetic moments, Fe, Co and Ni atoms are allowed to mix without producing any significant local magnetic disturbance; moreover, this experimentally observed broadening does not appear in corresponding Fe-Co and Fe-Ni alloys. In order to verify the homogeneous incorporation of carrier-free ^{57}Co in an Ni host, two samples containing 0.1% and 1% carrier Co (no. VI-VII in table 2) have been prepared under identical conditions. Their identical Mössbauer spectra are similar to those of carrier-free samples. Within experimental error, identical values of the magnetic field allow us to reject the assumption of ^{57}Co : Co micro-domains agglomerating in the Ni matrix. At RT, the average value of H in ^{57}Co : Ni is equal to 267 ± 5 kOe, in agreement with other kinds of samples in which the dopant species has been introduced by various ways such as electrodeposition [13] or proton irradiation [14].

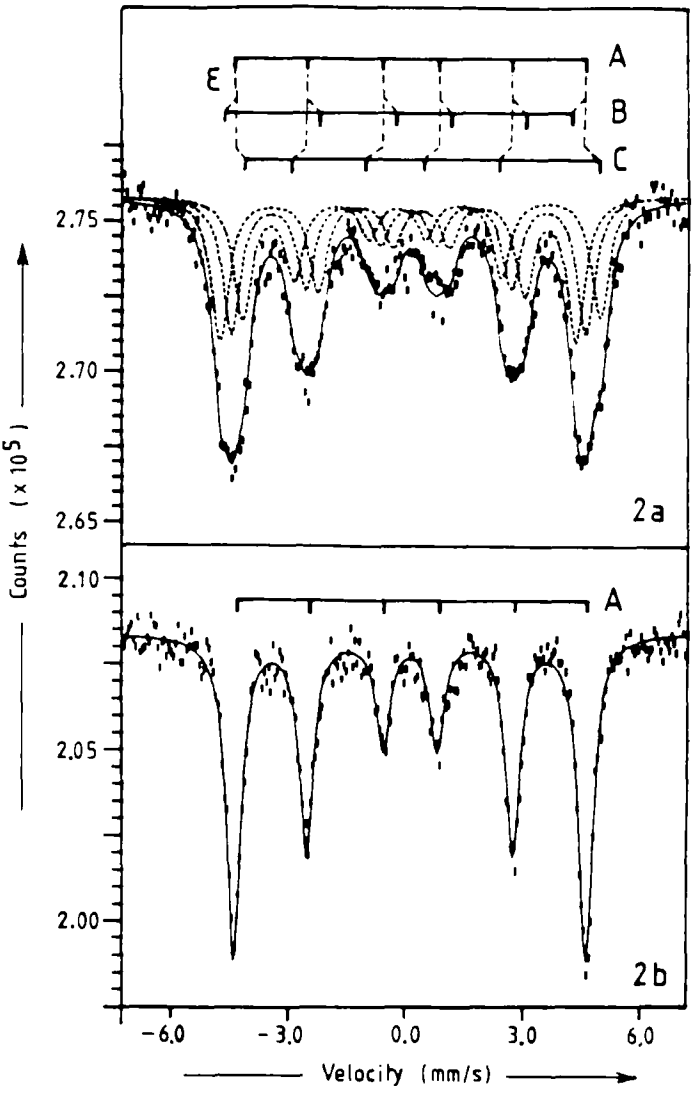

Fig. 2. Emission Mössbauer spectra at 90 K of ^{57}Fe in ^{57}Ni : Ni (sample B; T_D = 77 K): (a) before and (b) after annealing at RT.

4.3. ^{57}Ni : Ni

Mössbauer emission parameters for ^{57}Fe in ^{57}Ni-labelled Ni are listed in table 3; examples of Mössbauer spectra (sample B) are shown in fig. 2. The initial Mössbauer emission spectrum of ^{57}Fe, recorded at 90 K after total decay of ^{57}Ni in liquid nitrogen, exhibits an unusual shape (fig. 2a). The rather complex magnetic structure may be roughly regarded as an abnormally broadened magnetic sextet (Γ = 0.90 – 1.58 mm.s^{-1}).

Table 3

Emission Mössbauer parameters of ^{57}Fe in ^{57}Ni-labelled nickel (^{57}Ni : Ni)

Sample[a]	T_D[c] (K)	T_A[c] (K)	T_S[c] (K)	ϵ[d] (mm/s)	δ^{Fe} (mm/s)	Γ[e] (mm/s)	H (kOe)	I (%)
A + [b]	77	-	90	-	0.08	1.58	277	100
+ [b]	77	-	90	0.01	0.08	0.45*	277	30
				− 0.44	0.09	0.45	276	37
				0.50	0.07	0.45	279	33
+ [b]	77	-	90	0.01	0.08	0.74	276	24
				− 0.41	0.08	0.74	277	42
				0.48	0.07	0.74	279	34
	77	295	90	-	0.09	0.45	279	100
	77	295	295	-	− 0.02	0.55	263	100
	77	520	90	-	0.10	0.44	280	100
	77	520	295	-	− 0.02	0.50	268	100
	77	1070	90	-	0.10	0.53	283	100
	77	1070	295	-	0.00	0.51	273	100
B + [b]	77	-	90	-	0.10	0.93	281	100
+ [b]	77	-	90	0.00	0.09	0.55	281	34
				− 0.30	0.11	0.55	282	36
				0.31	0.11	0.55	283	30
[f]	77	-	90	-	0.09	0.49	279	100
	77	295	90	-	0.09	0.44	278	100
	77	295	295	-	− 0.01	0.39	268	100

[a] Sample A: ^{57}Ni : $NiC_2O_4.2H_2O$ heated at 450 °C under argon; decay time at 77 K: 20 days, analysis time at 90 K: 15 days.
[b] Sample B: ^{57}Ni : $NiC_2O_4.2H_2O$ heated at 600 °C under argon; decay time at 77 K: 34 days, analysis time at 90 K: 14 days.
[b] Sign + indicates the alternative fits of same initial data.
[c] T_D = decay temperature (^{57}Ni → ^{57}Co); T_A = annealing temperature; T_S = Mössbauer source temperature.
[d] $\epsilon = (e^2qQ/8)(3\cos^2\theta - 1)$.
[e] The asterisk (*) indicates a fixed parameter.
[f] Second analysis at 90 K after three months storage in liquid nitrogen.

This broadening disappeared completely in a second measurement at 90 K, after the sample had been warmed to RT (fig. 2b). Moreover, further experiments indicated that this "recovering effect" may even occur at 77 K, provided the storage in liquid nitrogen has been extended to a few months. Heating above RT does not induce any other effects.

Table 3 summarizes the Mössbauer parameters associated with two different samples, A and B. For each of the initial low-temperature spectra, two or more alternative fits (indicated by +) have been proposed to account for the experimental data. The first one corresponds to the structure mentioned earlier, i.e. a very broad sextet. The other ones superimpose three Zeeman sextets of equal magnetic fields, isomer shifts and line widths, together with a quadrupole splitting, in agreement with the recoil model proposed hereafter.

5. Discussion

5.1. RECOIL MODEL APPLIED TO ^{57}Ni : Ni

The main question arises as to whether or not the ^{57}Co atoms are effectively displaced by nuclear recoil during the ^{57}Ni decay. Referring back to the energetic aspects (sect. 2), and assuming a mean value for the displacement threshold energy of 15 to 25 eV, displacement of nucleogenic ^{57}Co atoms seems highly probable at least in 60% of the nuclear events. The model here proposed assumes the actual recoil of ^{57}Co in the Ni host lattice and predicts its consequences as to the behaviour before and after recovery.

(1) Initial amounts of ^{57}Ni atoms in the labelled material are very low (10^{-5} to 10^{-6} % at.) and comparable with the natural content of Schottky defects in the matrix, so there is a low probability for close neighbouring of radioactive precursors and vacancies. The upper part of fig. 3 represents the initial view of a (111) plane where ^{57}Ni atoms and vacancies are randomly distributed in the lattice.

(2) When the ^{57}Co nucleogenic atom recoils in the lattice, it initiates a replacement collision chain leading to the appearance of a vacancy at the initial ^{57}Ni site, and of an interstitial Ni atom at some atomic distances from the previous one. This so-called Frenkel pair is however highly unstable unless both partners are separated by a minimum distance depending on its orientation with respect to the crystal axes. Practically, the replacement collision ends in the surroundings of a pre-existing vacancy, which is then occupied by the terminal atom of the collision chain. The immediate transfer of a recoiling ^{57}Co atom into an interstitial position is most unlikely: firstly, because of the stronger sterical hindrance due to the larger size of Co (r = 126 pm) than Ni (r = 124 pm) and secondly, because of the very low stability of the corresponding Frenkel pair.

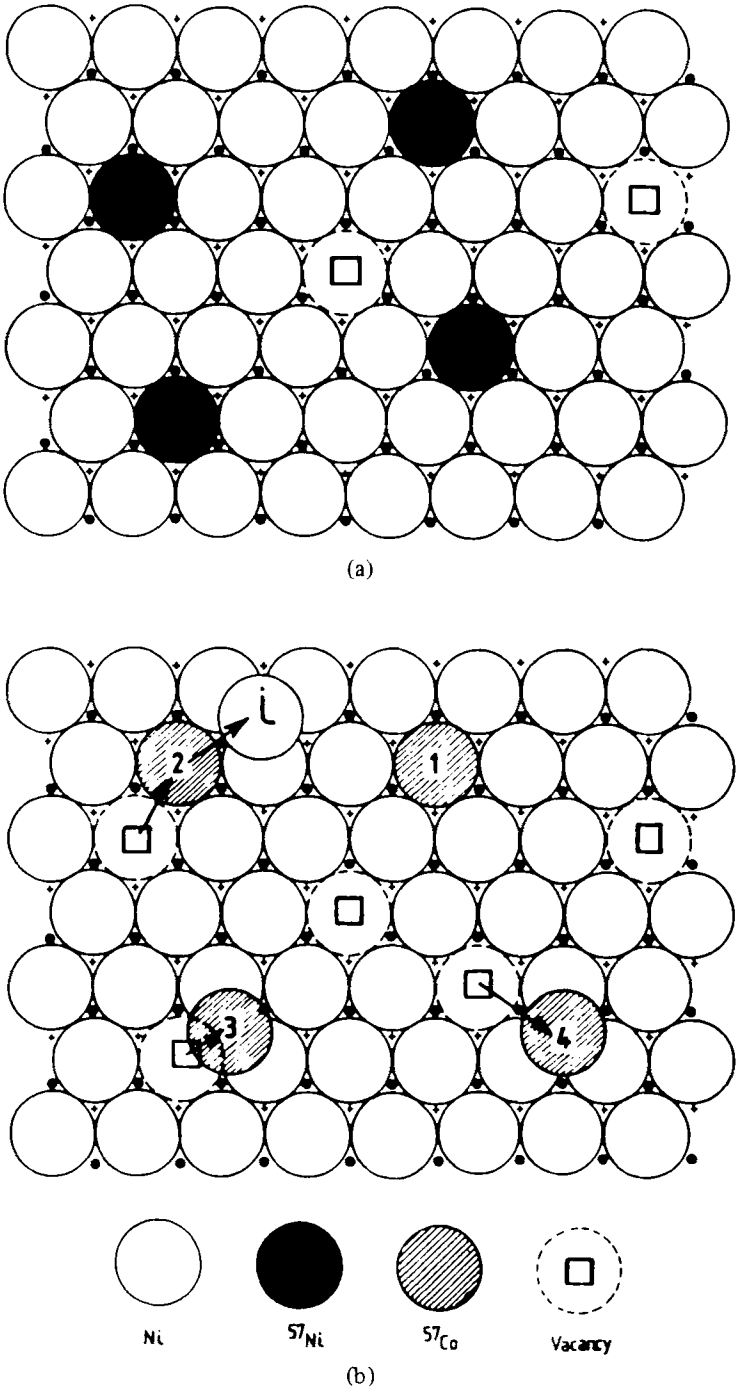

Fig. 3. ^{57}Co recoil sites in a (111) plane of ^{57}Ni : Ni; (a) before and (b) after recoil.

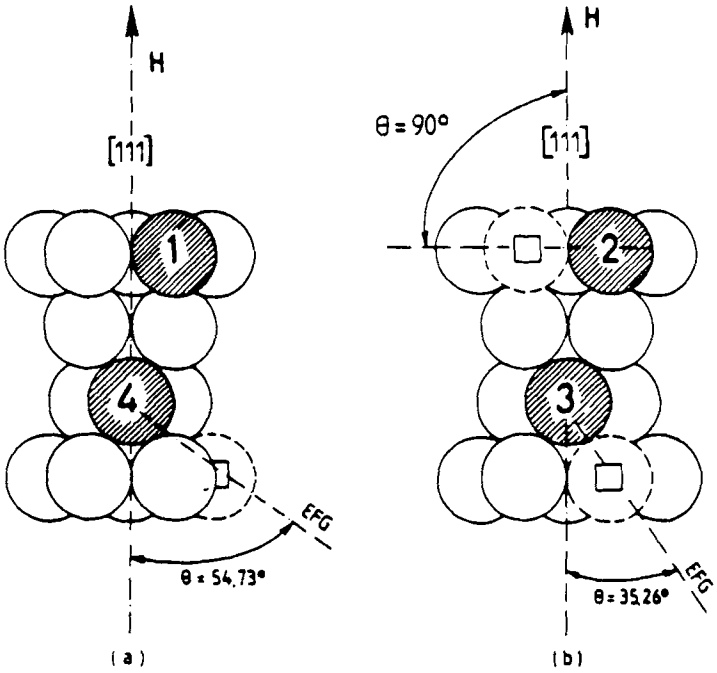

Fig. 4. ^{57}Co recoil sites in ^{57}Ni : Ni; relative orientation of V_{ZZ} (EFG) with respect to the magnetic field axis.

Table 4

Structural data of the different recoil sites

Site number[a]	Recoil direction	θ [b]	$3\cos^2\theta - 1$	$d_{\square}/^{57}$Co[c]
1	-	-	-	-
2	⟨110⟩	90°	− 1.00	$0.707a$
3	⟨110⟩	35.26°	+ 1.00	$0.707a$
4	⟨100⟩	54.73°	0.00	a

[a] According to figs. 3 and 4.
[b] Angle between H and V_{ZZ}.
[c] Distance separating the vacancy from the Mössbauer probe;
a = lattice constant (352 pm).

(3) The following sequences must now be considered (fig. 3b):

(a) No recoil ($E_R < E_d$), or displacement followed by a return into the initial position. Energy is then dissipated by vibration around the normal lattice site. Concerned ^{57}Co atoms are found in substitutional positions, surrounded by a normal and complete coordination sphere, so that these will be called "normal sites" (no. 1 in fig. 3b).

(b) Displacement in the close-packed layer along ⟨110⟩; this results in a substitutional ^{57}Co atom next to the created vacancy situated in the same crystal plane (no. 2 in fig. 3b).

(c) Displacement to a neighbouring (111) layer, above or below, but parallel to the one which contained the ^{57}Co atom, either

- along ⟨110⟩ to one of the six nearest-neighbours (no. 3 in fig. 3b), or
- along ⟨100⟩ to a second nearest-neighbour (no. 4 in fig. 3b).

Both cases give rise to ^{57}Co atoms next to a vacancy belonging to an adjacent (111) plane, but at different distances.

(4) The occurrence of a vacancy next to the ^{57}Co atom destroys the cubic symmetry around the Mössbauer probe and induces an electric field gradient (EFG) with axial symmetry. This results in a quadrupole splitting whose value depends on (i) the EFG's magnitude, characterized by its largest component V_{ZZ}, and (ii) the relative orientation θ of V_{ZZ} with respect to the internal magnetic field axis, according to:

$$\Delta = 2\epsilon = (1 - \gamma_\infty) \frac{eQV_{ZZ}}{4} (3\cos^2\theta - 1) .$$

(5) According to the anisotropic character of the magnetocrystalline energy in ferromagnetic materials, nickel has eight equivalent directions of easy magnetization, corresponding to ⟨111⟩ directions at RT [15] and changing to ⟨110⟩ above 490 K [16]. In a demagnetized crystal of nickel not subjected to external strains, one eighth of the Weiss domains are thus oriented along each of these easy directions.

(6) For each situation considered above (see fig. 4), the magnitude of the quadrupolar perturbation ϵ may be estimated using the data of table 4. The model suggests the following comments:

- A fortuitous cancellation of the quadrupole splitting would normally make site 4 indistinguishable from site 1, but its formation may be excluded in accordance with energetic conditions for ⟨100⟩ displacement (see sect. 2).
- The quadrupole splittings of sites 2 and 3 are equal in magnitude but of opposite signs due to the angular term. Because of equal statistical probabilities for ^{57}Co to collide with one of the twelve nearest-neighbouring atoms, both sites 2 and 3 have also to appear with equal probabilities, within the limits of perfectly fulfilled energy requirements.

5.2. INTERPRETATION OF THE LOW TEMPERATURE SPECTRUM BEFORE ANNEALING

On the basis of the above model, the Mössbauer spectrum at 90 K obtained before annealing (fig. 2a) has been resolved in three superimposed Zeeman sextets having (i) identical magnetic hyperfine fields ($H \cong 280$ kOe), (ii) identical isomer shifts, (iii) similar relative intensities ($\sim 33\%$), and (iv) quadrupolar interactions which are equal in magnitude but of opposite signs. Sextet A corresponds to the "normal site" ($\epsilon_A = 0$); assuming a negative sign for V_{ZZ}, a positive value of ϵ means a negative angular term, so that sites B ($\epsilon_B = -0.30$ mm.s^{-1}) and C ($\epsilon_C = +0.31$ mm.s^{-1}) are related to sites 3 and 2, respectively (see table 4 and fig. 4). Obtaining a $|\epsilon_B/\epsilon_C|$ ratio close to unity and equivalent amounts of both non-cubic sites agrees well with the proposed recoil model. The total fraction of recoil species observed at 90 K reaches about 65%, which is in agreement with energetic considerations (see sect. 2). This may be compared with the observation, by means of radiochemical studies, of a 37% retention in ^{57}Ni-labelled nickel phtalocyanine [17,18]. The present results may also be compared to a recent report of PAC studies on the $^{111}\text{Sn} \rightarrow {}^{111}\text{In} \rightarrow {}^{111}\text{Cd}$ decay in a Cu metal host; at 4 K, single Frenkel pairs are detected which are ascribed to recoil species ($E_R = 29$ eV) due to neutrino and γ-ray emission [19]. The interpretation of these experiments has however given rise to some controversy [20].

5.3. RECOVERY BEHAVIOUR

In a further Mössbauer measurement at 90 K, either a prolonged storage at 77 K or after warming to RT, the experimental broadening of lines completely disappears, while the mean value of H remains constant (fig. 2b). This indicates that all the radiative defects are then completely healed as a result of vacancy diffusion. Such behaviour has to be looked upon in the light of defect mobility and corresponding activation energies for migration. The time-dependent concentration C of a given defect is usually expressed as:

$$\frac{dC}{dt} = -F(C) \cdot \nu \cdot e^{-E_m/kT} ,$$

where $F(C)$ is a function of concentration, ν the lattice vibration frequency ($\cong 10^{12}$ s^{-1}), and E_m the activation energy for defect migration. Typical values of E_m in Ni are 1.4 eV for a vacancy [21] and 0.1–0.3 eV for an interstitial [4]. These values allow us to explain the isochronal recovery curves of various metals after low-temperature irradiations with electrons [1,6,7,22,23] or fast neutrons [1,24–26]. Typical results obtained for nickel samples which have been heated for successive 10 minute periods show that a partial recovery is initiated in the temperature range 30–40 K, and that the recovery rate reaches about 65% in the range 60–90 K [6].

Extended curves up to RT indicate a total recovery. It may therefore be concluded that under the present working conditions, internal radiation damage is continuously annealed, first and partly during the ^{57}Ni decay at 77 K, and later, slightly faster, during the Mössbauer measurement at 90 K. The initial emission spectrum shows a perturbed state changing to a normal environment. This is seen by the enhancement of the intensity of the central sextet A at the expense of the intensities of the external ones, which results in decreasing line widths. This also accounts for the observation of a normal emission spectrum at 90 K for sample B, after the latter had been stored at 77 K for three months.

Moreover, neglecting the stabilization of Frenkel pairs, the recoil model is consistent with the very low E_m values for interstitials. In the same way, a parallel argument has also been given by simulation techniques indicating that, even at low temperatures, most of the Frenkel pairs annihilate during the collision chain itself [27,28]; this occurs in any case where a very low energy such as 0.1 eV is available [29]. These theoretical predictions have been experimentally verified and the role of interstitials in the first stages of the isochronal thermal annealing has become evident.

6. Conclusions

Conducting materials are appropriate systems to detect atomic recoil as a result of high-energy neutrinos and γ-ray emissions accompanying a nuclear decay in the solid state. Evidence for the recoil of nucleogenic ^{57}Co atoms has been given by ^{57}Fe emission Mössbauer spectroscopy in ^{57}Ni-labelled Ni, when the ^{57}Ni decay and the subsequent Mössbauer analysis are both performed at low temperature. Heating to RT or prolonging the storage at 77 K for several months causes complete annealing. Experimental data are interpreted in the light of a recoil model and a recovery behaviour. Agreement is observed with:

- the energetics of the ^{57}Ni $\rightarrow$ ^{57}Co $\rightarrow$ ^{57}Fe decay,
- the typical threshold energy values for atomic displacement in Ni, and
- the relative mobilities, as a function of temperature, of Schottky and Frenkel defects in such systems.

In the non-annealed sample, recoil ^{57}Co atoms are always found in substitutional positions, either in normal sites having a cubic symmetry, or in two different vacancy-associated sites where the magnetic interaction is perturbed by quadrupole splittings due to the non-cubic symmetry.

Acknowledgements

The authors are very grateful to the operating staff of the Cyclotron of Louvain-la-Neuve for technical support, and to the Institut Interuniversitaire des Sciences Nucléaires for financial assistance.

References

[1] T. Wichert, Hyp. Int. 15/16(1983)335.
[2] G. Vogl, Hyp. Int. 2(1976)151.
[3] H. de Waard, Phys. Scripta 11(1975)157.
[4] H. Bernas, Phys. Scripta 11(1975)167.
[5] R.L. Auble, Nucl. Data Sheets 20(1977)327.
[6] P.G. Lucasson and R.M. Walker, Phys. Rev. 127(1962)485.
[7] P. Vajda, Rev. Mod. Phys. 49(1977)481.
[8] F.J. Haasbroek, J. Steyn, R.D. Neirinckx, G.F. Burdzik, M. Cogneau and P. Wanet, Council for Scientific and Industrial Research report CSIR-FIS89 (1976).
[9] G.N. Rao, Hyp. Int. 7(1979)141.
[10] F.M. Galperin, Phys. Stat. Sol. (b) 57(1973)715.
[11] G.K. Wertheim and J.F. Wernick, Phys. Rev. 123(1961)755.
[12] C.E. Johnson, M.S. Ridout and T.E. Cranshaw, Proc. Phys. Soc. 81(1963)1079.
[13] A. Vertes, Z. Kajcsos, I. Czako-Nagy, M. Lakatos-Varsanyi, L. Czordas, G. Brauer and H. Leidheiser, Nucl. Instr. Meth. 199(1982)353.
[14] A.K. Zhetbaev, J. de Phys. 41(1980)C1-457.
[15] R.M. Bozorth, *Ferromagnetism* (D. Van Nostrand Comp. Inc., Princeton, 1963) p. 478.
[16] G. Ghandra and T.S. Radhakrishnan, Phys. Lett. 28A(1968)323.
[17] M.H. Yang, K. Yoshihara and N. Shibata, Radiochim. Acta 15(1971)17.
[18] J.L. Thompson, J. Ching and E.Y. Fung, Radiochim. Acta 18(1972)57.
[19] H. Metzner, R. Sielemann, R. Butt and S. Klaumunzer, Phys. Rev. Lett. 53(1984)290.
[20] W. Frank, Radiat. Eff. Lett. 87(1985)1.
[21] G. Vogl, J. de Phys. 35(1974)C6-165.
[22] F. Maury, A. Lucasson and P. Lucasson, Cryst. Lett. Defects 2(1971)47.
[23] K. Forsch, J. Hemmerich, H. Knoll and G. Lucki, Phys. Stat. Sol. (a) 23(1974)223.
[24] W. Mansel and G. Vogl, J. Phys. F7(1977)253.
[25] W. Mansel, J. Marangos and D. Wahl, J. Nucl. Mater. 108/109(1982)137.
[26] M. Kobiyama and S. Takamura, Radiat. Eff. 84(1985)161.
[27] D.G. Doran, Radiat. Eff. 2(1970)249.
[28] A.J. Foreman, Radiat. Eff. 21(1974)81.
[29] K. Drittler, H.J. Lahmann and H. Wollenberger, Radiat. Eff. 2(1969)51.